frontiers in Marine Science

TYPE Original Research
PUBLISHED 24 March 2026
DOI 10.3389/fmars.2026.1757436



OPEN ACCESS

EDITED BY
Giuseppe Suaria,
National Research Council, Italy

REVIEWED BY
David Mendes,
Federal University of Rio Grande do Norte, Brazil
Margaret Murakami,
The University of Texas at Austin, United States

*CORRESPONDENCE
Luuk Rader
luukrader@gmail.com
Borja Aguiar-González
borja.aguiar@ulpgc.es

RECEIVED 30 November 2025
REVISED 12 February 2026
ACCEPTED 17 February 2026
PUBLISHED 24 March 2026

CITATION
Rader L, Aguiar-González B, Price TD, Vega-Moreno D, Fraile-Nuez E and Machín F (2026) Oceanward surface transport from the NW African upwelling zone by coastal jet detachment and filaments. *Front. Mar. Sci.* 13:1757436. doi: 10.3389/fmars.2026.1757436



# Oceanward surface transport from the NW African upwelling zone by coastal jet detachment and filaments

Luuk Rader[1]*, Borja Aguiar-González[2]*, Timothy David Price[3], Daura Vega-Moreno[4], Eugenio Fraile-Nuez[5] and Francisco Machín[6]

[1]Department of Earth Sciences, Faculty of Geosciences, Utrecht University, Utrecht, Netherlands, [2]EOMAR, University Institute for Sustainable Aquaculture and Marine Ecosystems (IU-ECOAQUA), Universidad de Las Palmas de Gran Canaria, Las Palmas, Spain, [3]Department of Physical Geography, Faculty of Geosciences, Utrecht University, Utrecht, Netherlands, [4]OpenPLAS Group, Chemistry Department, Universidad de Las Palmas de Gran Canaria (ULPGC), Las Palmas de Gran Canaria, Spain, [5]Spanish Institute of Oceanography (IEO), Spanish National Research Council (CSIC), Las Palmas de Gran Canaria, Santa Cruz de Tenerife, Spain, [6]Oceanografía Física y Geofisica Aplicada (OFYGA), University Institute for Sustainable Aquaculture and Marine Ecosystems (IU-ECOAQUA), Universidad de Las Palmas de Gran Canaria, Las Palmas de Gran Canaria, Spain

The oceanward surface transport of particles, including marine litter, from the northwestern African upwelling zone is influenced by multiple interacting physical processes. This study applies the OceanParcels Lagrangian framework to investigate the mechanisms that may contribute to oceanward surface transport in this region, motivated by the hypothesis that the northwestern African upwelling system could represent a potential source of marine litter in the vicinity of the Canary Islands. The simulations suggest that the coastal jet stream and its detachment, upwelling filaments, and Stokes drift play key roles in shaping particle trajectories. In particular, coastal jet detachment appears to organize surface transport into narrow, oceanward-oriented particle corridors, while upwelling filaments may provide additional offshore export pathways. Stokes drift introduces a predominantly southward deflection that can reduce or modulate oceanward advection and enhance alongshore transport. These results provide a process-based, model-derived first assessment of previously understudied oceanward transport corridors in the NW African upwelling system. They are consistent with the hypothesis that this region may contribute to surface tracer transport toward the Canary Islands. However, caution is required when extrapolating these findings to marine debris, as windage is not included and may significantly alter transport pathways. Continued investigation, including observational validation and improved surface forcing representations, will help further constrain the mechanisms shaping particle transport in the NW African upwelling system.

KEYWORDS

**Lagrangian tracking, NW African upwelling, oceanward transport, particle corridors, reanalysis products**

# 1 Introduction

Amidst the global challenge of plastic pollution, the Canary Islands are one of the areas most affected by the accumulation of marine plastic debris transported by ocean currents. Most plastic debris at or near the islands is likely to have an exogenous origin and is expected to be transported by the dominant southward flowing currents near the islands (Baztan et al., 2014; Cardoso and Caldeira, 2021; Hernández-Sánchez et al., 2021; Villanova-Solano et al., 2022). As an example, an issue caused by this pollution is the entanglement in abandoned fishing gear as a major death cause for sea turtles, contributing to values of mortality of 25% or greater (Orós et al., 2005).

The Canary Islands are located in the Atlantic Ocean at about 28°N and about one hundred kilometers west off the northwestern African coast (Figure 1). Driven by the north-eastern trade winds, this coast presents one of the four major upwelling regions in the world (Valdés and Déniz-González, 2015), bringing North Atlantic Central Water into the euphotic zone (Lathuilière et al., 2008). The Canary Current System (CCS) consists of two dominant southward flowing currents: the Canary Current (CC), constituting the eastern boundary current of the North Atlantic Subtropical Gyre (Machín et al., 2006), and the Canary Upwelling Current (CUC), a coastal jet stream formed along the cold upwelling front (Pelegrí et al., 2005). In addition, the CCS exhibits many mesoscale features increasing the versatility of currents in this region. Upwelling filaments, also known as cold-water tongues originating from upwelling regions, play a critical role in transporting mass and organic carbon toward the open ocean (Barton et al., 1998; Nieto et al., 2012; Sangrà et al., 2015; Santana-Falcón et al., 2020). Furthermore, the presence of the Canary Islands disturbs currents and leads to the formation of mesoscale eddies (Arístegui et al., 1994; Barton et al., 1998). The intensity of upwelling also varies seasonally, reaching its peak during spring and summer (Benazzouz et al., 2014).

Over the past decade, Lagrangian particle tracking has become a widely used and powerful tool to investigate oceanic transport pathways of tracers such as larvae, pollutants, and floating marine debris. Numerous studies have demonstrated that short- to medium-term particle tracking can reveal coherent transport structures, source–sink relationships, and accumulation zones that are not easily inferred from Eulerian velocity fields alone (Mason et al., 2012; Maximenko et al., 2012; van Sebille et al., 2018; Iskandar et al., 2022; Vega-Moreno et al., 2024).

In particular, Lagrangian approaches have proven highly valuable for studying the dispersion and fate of floating plastics at both regional and basin scales, highlighting the dominant role of mesoscale and submesoscale circulation in shaping transport pathways (van Sebille et al., 2018; van Sebille et al., 2020). These methods provide a physically intuitive framework to link ocean circulation features to observed tracer distributions, and they are now routinely applied to assess connectivity patterns, offshore export mechanisms, and accumulation regions across the global ocean.

In the Canary Current System and the NW African upwelling region, previous studies have extensively documented the presence of coastal upwelling jets, mesoscale eddies, and recurrent upwelling filaments that export water, nutrients, and organic matter offshore (Arístegui et al., 1994; Barton et al., 1998; García-Muñoz et al., 2004; Pelegrí et al., 2005; Troupin et al., 2012; Santana-Falcón et al., 2020). These studies, based on Eulerian velocity fields, hydrographic observations, and satellite SST or chlorophyll imagery, have established that filaments and eddies play a major role in cross-shelf exchange and offshore transport in this region. In particular, upwelling filaments originating near major capes such as Cape Ghir have long been recognized as important offshore export pathways for water masses and biogeochemical tracers. However, most of this work has focused on water-mass properties, nutrient and carbon export, or biogeochemical variability, rather than on explicit Lagrangian particle pathways. As a result, while the dynamical structures responsible for offshore export are well known in an Eulerian or observational sense, their role in organizing surface particle transport into coherent offshore pathways has received comparatively little attention.

Despite this extensive body of work, the explicit identification of coherent oceanward surface particle pathways from the NW African coast using Lagrangian simulations has received little attention. While upwelling filaments have long been recognized as offshore export mechanisms, the organization of surface particle transport into narrow, quasi-persistent oceanward corridors linked to coastal jet detachment has not, to our knowledge, been demonstrated in this region using Lagrangian tracking.

Recent Lagrangian studies have started to explore plastic transport toward Macaronesia using numerical simulations and observational tags (Sala et al., 2013; Cardoso and Caldeira, 2021; Cividanes et al., 2024). These studies provided important insights into large-scale connectivity patterns and source–sink relationships for marine litter reaching the Canary Islands. However, they focused primarily on basin-scale or regional connectivity, rather than on identifying the physical formation mechanisms of coherent offshore transport pathways in the NW African upwelling zone itself.

The present study addresses this gap by combining high-resolution reanalysis products with Lagrangian particle simulations to (i) identify coherent oceanward surface transport pathways from the NW African coast, (ii) isolate the relative roles of wind-driven circulation, geostrophic flow, and Stokes drift in shaping these pathways, and (iii) assess how these mechanisms jointly modulate the offshore export of passive tracers from the NW African upwelling region toward the open ocean and the Canary Islands.

Below, the methodology is detailed in section 2, explaining the Lagrangian particle-tracking setup, the ocean and wave products and the experiments applied in this study. Section 3 presents the results of this study by showing particle distributions and trajectories, identifying oceanward corridors, upwelling filaments and the impact of Stokes drift. Section 4 discusses the formation mechanism of the corridors and the role of upwelling filaments on oceanward transport, evaluates the influence of Stokes drift, and presents limitations of this study. Finally, Section 5 concludes the main findings on oceanward transport pathways, their seasonality and their drivers.

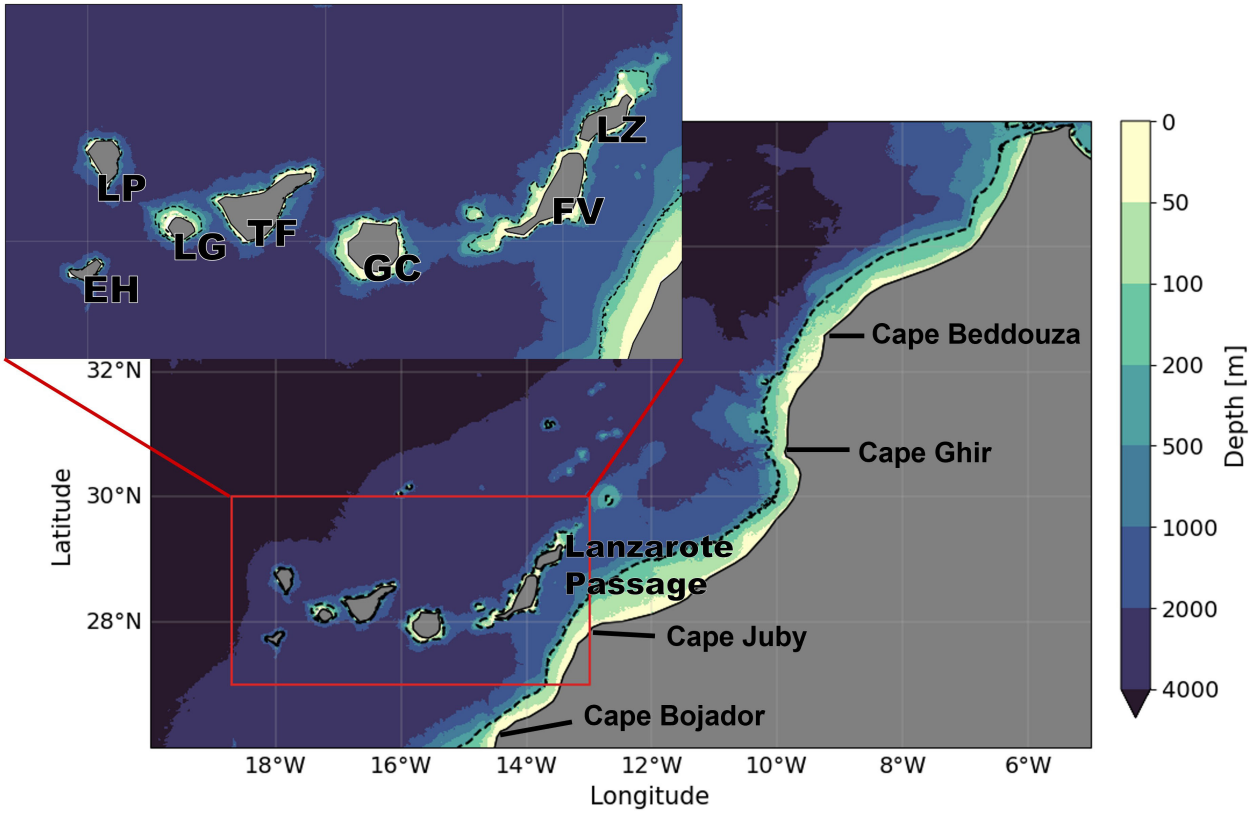


FIGURE 1
A bathymetric map of the study domain, with indication to the major capes along the African coast and the Canary Islands. The abbreviations corresponding to the Canary Islands are defined as follows: LZ, Lanzarote; FV, Fuerteventura; GC, Gran Canaria; TF, Tenerife; LG, La Gomera; LP, La Palma; EH, El Hierro. Furthermore, the 200 m isobath approximately represents the location of the shelf break.

# 2 Methods

## 2.1 Lagrangian tracking

This study utilized OceanParcels v2.0, a Lagrangian simulator designed for tracking both passive and active particles (Lange and van Sebille, 2017; Delandmeter and van Sebille, 2019). The trajectories of the particles are equivalent to solving the subsequent equation:

$$\vec{x}(t+\Delta t) = \vec{x}(t) + \int_{t}^{t+\Delta t} \vec{v}(\vec{x}, \tau) d\tau + \Delta X_b(t) \quad (1)$$

where $\vec{x}$ is the two-dimensional position of the particle and $\vec{v}(\vec{x}, \tau)$ is the velocity of the particle at this position during modeling time step $\tau$, obtained through linear interpolation of the surface velocity data. $\Delta X_b(t)$ represents the change in position due to the "behavior" of the particle. However, given this study considered passive particles, advected by oceanic dynamics only, this term can be neglected.

In this study, the built-in RK4-kernel the OceanParcels was employed, which solves Equation 1 using a fourth order Runge-Kutta discretization (Lange and van Sebille, 2017), using a modeling time step of one hour and an output time step of one day. To minimize the likelihood of particles becoming trapped along the shoreline, the built-in free-slip function of OceanParcels was applied.

## 2.2 Ocean products

The velocity fields from different ocean products were used as input for the simulations conducted with Ocean Parcels. This was done to evaluate the influence of different oceanographic aspects, such as geostrophy and Stokes drift, on the oceanward transport of particles. The properties of these products are detailed in this section. All products were sourced from the Copernicus Marine Environment Monitoring Service (CMEMS). A summary of the utilized products is provided in Table 1.

For the general ocean circulation data, the CMEMS Global Ocean Physics Reanalysis product (GLORYS12V1, hereafter referred to as GLORYS) (Lellouche et al., 2018) and the CMEMS Iberian-Biscay-Irish Ocean Physics Analysis and Forecast product (IBI-OP) (Aznar et al., 2016) were used. Both are eddy-resolving products derived from the Nucleus for European Modeling of the Ocean (NEMO) model (Madec and the NEMO System Team, 2024). Due to its high resolution, which captures (sub-)mesoscale variability most effectively, IBI-OP served as the primary product for this study. GLORYS was used to validate the features identified by IBI-OP, leveraging its extended temporal coverage to provide climatologically averaged surface current data.

To differentiate between geostrophic and wind-driven surface dynamics, two additional products were employed: the AVISO altimetry product (Chiswell and Rickard, 2008) and the GlobCurrent product (Rio et al., 2014). AVISO provides

TABLE 1 An overview of the ocean products used in this study.

| Flow field | Product | Spatial resolution | Period (full years) | Source |
|---|---|---|---|---|
| General circulation | GLORYS reanalysis | 1/12° | 1993 - 2020 | Lellouche et al. (2018) |
| General circulation | IBI-OP analysis and forecast | 1/36° | 2022 | Aznar et al. (2016) |
| Geostrophic velocities | AVISO reanalysis | 1/8° | 1993 - 2022 | Chiswell and Rickard (2008) |
| Geostrophic + Ekman velocities | GlobCurrent reanalysis | 1/4° | 2007 - 2022 | Rio et al. (2014) |
| Stokes drift | IBI-OW analysis and forecast | 1/20° | 2021 - 2022 | Toledano et al. (2022) |

geostrophic surface velocities derived from multi-satellite observations of sea level anomalies. In contrast, GlobCurrent integrates geostrophic currents with modeled Ekman currents, utilizing wind stress data from the ECMWF ERA wind products (Hersbach et al., 2020).

To account for the displacement of particles by Stokes drift, two wave reanalysis products were used: WAVERYS (Law-Chune et al., 2021) and IBI-OW (Toledano et al., 2022). Both products are derived from the MFWAM wave model and are driven by wind stress from ECMWF, along with surface velocities from GLORYS and IBI-OP respectively. Consequently, the Stokes drift velocity field from WAVERYS is combined with the GLORYS velocity field, while the Stokes drift velocity field from IBI-OW is added to the IBI-OP velocity field.

The approach of adding a wave product to general circulation data has been applied in studies such as Cardoso and Caldeira (2021) and Iskandar et al. (2022). However, it is important to note that the methodology of incorporating Stokes drift onto general circulation data remains an active area of research. As argued by Higgins et al. (2020) and Cunningham et al. (2022), summing up Stokes drift with the general surface velocities likely overestimates the influence of Stokes drift, as is also the case for this study. Furthermore, the impact of Stokes drift on the trajectories of marine debris depends on its size as well, since bigger (more buoyant) debris is likely to be influenced more by the depth-limited effect of wave action (Breivik et al., 2016; Van Den Bremer and Breivik, 2017). In this study, the full effect of Stokes drift is considered, serving as a preliminary exploration of its general impact on surface advection within the study region.

## 2.3 Particle set-up and simulations

In the simulations, particles were released within a release band based on offshore distance (Figure 2). The release followed a grid-like structure with a spatial resolution of 1/18°, extending within a maximum offshore distance of 1/3° and a minimum distance of 1/18° from the coast. The maximum distance was chosen to approximate the average width of the continental shelf, while the minimum distance prevented the particles from interfering with the coast immediately upon release. Particles were released between the latitudes of 22°N and 35.75°N, except when using the IBI products, due to their limited spatial domain. For the IBI products, particles were released between 27°N and 35.75°N.

Multiple experiments were conducted, each specifically designed to investigate a particular aspect of oceanward particle transport. These experiments are described in the following.

### 2.3.1 Seasonal mean ocean dynamics

A set of simulations were conducted using seasonal mean surface velocities to identify the primary and persistent features responsible for oceanward particle transport, excluding the influence of temporary (sub-)mesoscale variability. In this study, the (boreal) seasons are defined equally to the quarters of the year, thus winter consists of January, February and March, and so forth. This slight deviation from the astronomical or meteorological seasons was chosen to better align with the seasonal variability of the upwelling zone as indicated by the upwelling index calculated by Benazzouz et al. (2014).

Particles were released simultaneously and allowed to travel for 90 days in each simulation, corresponding to the approximate length of a season. The simulations were performed using the surface circulation data from the following oceanographic products: GLORYS, IBI-OP, AVISO, and GlobCurrent (Table 1).

To investigate the vertical structure of the features critical for the oceanward transport of particles, the same simulation was conducted using IBI-OP seasonal mean velocities, but with particles released at four different depth levels: 0, 22, 40 and 110 meters. Note that, although simulations incorporate multiple depths, only horizontal (two dimensional) velocity fields were employed to study the horizontal advection of particles, thus the vertical movement of particles was not included. In addition, for greater depth levels, particles were released further offshore rather than along the shoreline at the sea surface, considering the bathymetry of the region.

### 2.3.2 Daily varying surface velocities

To assess the impact of daily variability in (sub-)mesoscale dynamics on the oceanward transport of particles and to simulate ocean conditions as realistically as possible, a simulation with daily varying surface dynamics was conducted. This simulation used the IBI-OP product, which, due to its high resolution, provides the most accurate representation of (sub-)mesoscale features. No temporal averaging was applied, preserving the daily variability of the ocean product.

Particles were released every 5 days over the course of one year. Following this, the simulation continued for an additional year using the same surface velocity fields from 2022, ensuring that all particles have an equal lifespan. Each particle was assigned a fixed lifespan of 365 days, after which it was removed from the simulation. This methodology enables the identification of both initial transport pathways and longer-term redistribution of

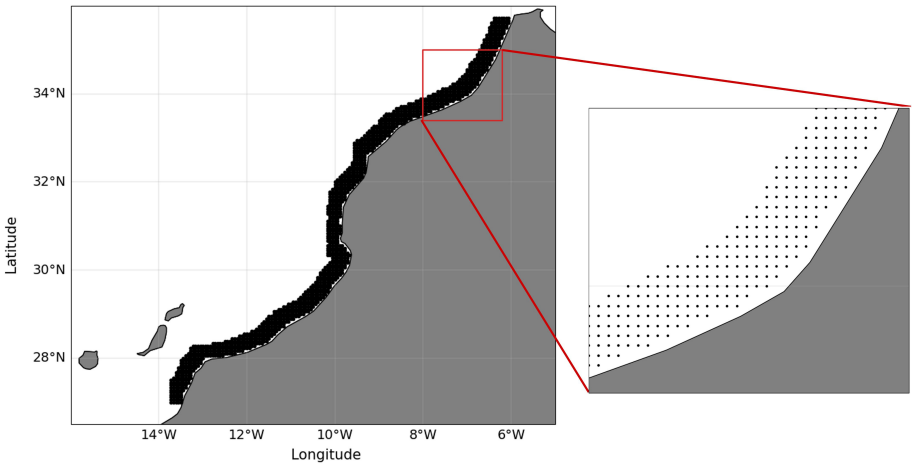


FIGURE 2
The initial position of particles released during the simulations using IBI-OP.

particles. A second simulation was performed by incorporating Stokes drift from IBI-OW into the IBI-OP general surface velocities. This approach enabled an evaluation of the combined effects of daily variability in general surface circulation and Stokes drift on particle transport.

# 3 Results

In the following section, the results obtained by the different experiments are presented. The results using seasonal mean ocean dynamics are presented (Section 3.1), followed by the results from the simulations using daily varying surface dynamics are presented, both including and excluding Stokes drift (Section 3.2).

## 3.1 Seasonal mean ocean dynamics

To highlight the main features driving oceanward particle transport, Figure 3 presents the Particle Distribution Plots (PDPs) from simulations using seasonal mean surface velocities from the IBI-OP model for the different seasons. These PDPs represent the fraction of the possible total particle count exhibited by each location, hence representing a normalized particle count for each location. Practically, a higher fraction within a grid cell indicates that a greater number of particles passed through it.

A prominent feature in Figure 3 is the emergence of two coherent oceanward-oriented corridors in the simulations, within which particles concentrate during oceanward transport. The northernmost corridor, typically well-defined in winter, spring, and summer, originates near Cape Beddouza at approximately 32.5°N. The second corridor generally originates near Cape Jubi, approximately at 28°N. The detachment of particles from the shore and the corridors from Cape Beddouza and Cape Jubi are highlighted in Figure 3 during the spring season. In contrast, the northernmost corridor is absent during autumn. Instead, a filament-like structure originating from Cape Ghir appears to dominate oceanward particle transport.

The corridors identified in the simulations generally span lengths on the order of a few hundred kilometers. Among them, the corridor originating north of Cape Beddouza is entirely contained within the IBI-OP domain and appears to be the most important pathway for oceanward particle transport, with potential implications for transport to the Canary Islands. As a result, this study will focus exclusively on this corridor from now on. Although this corridor originates near Cape Beddouza, Cape Ghir is more broadly recognized in literature (Troupin et al., 2012; Valdés and Déniz-González, 2015). Therefore, this corridor will be referred to as the Cape Ghir Corridor.

To quantitatively describe the Cape Ghir Corridor, key parameters describing its features are presented in Table 2. As an indication of upwelling intensity, the estimated maximum speed of the coastal jet stream located just north of the corridor is also depicted in Table 2. These values are estimated by plotting the velocity of particles released between 33°N and 35°N against their longitudinal positions. This specific subset of particles is chosen because they are released north of Cape Beddouza and are most likely to be transported via the jet stream. As an example, Figure 4a illustrates the particle speed as a function of longitude using the IBI-OP seasonal mean surface velocities for summer. Annotations in the figure highlight the methodology used to estimate the speed from such plots. The maximum speed of the coastal jet is derived by visually estimating the mean speed at the longitude where the particles are transported fastest, whereas the speed of the corridor is derived by visually estimating the mean velocity of the particles in the corridor. Additionally, the detachment angle (the angle between the parallels, defined as lines of equal latitude, and the mean strike of the corridor) is included in Table 2 and represented in Figure 4b.

Table 2 highlights that the maximum speed the coastal jet speed aligns with the seasonal variability of upwelling intensity in the region, with highest values observed during spring and summer. Correspondingly, the speed of the corridors increases during these seasons, reflecting enhanced oceanward transport. Also, the Rossby numbers higher than 1 indicate a non-purely geostrophic origin of these corridors. Table 2 also includes numerical descriptions of the corridors derived from simulations using the GLORYS seasonal mean surface circulation. These simulations agree, with further

10.3389/fmars.2026.1757436

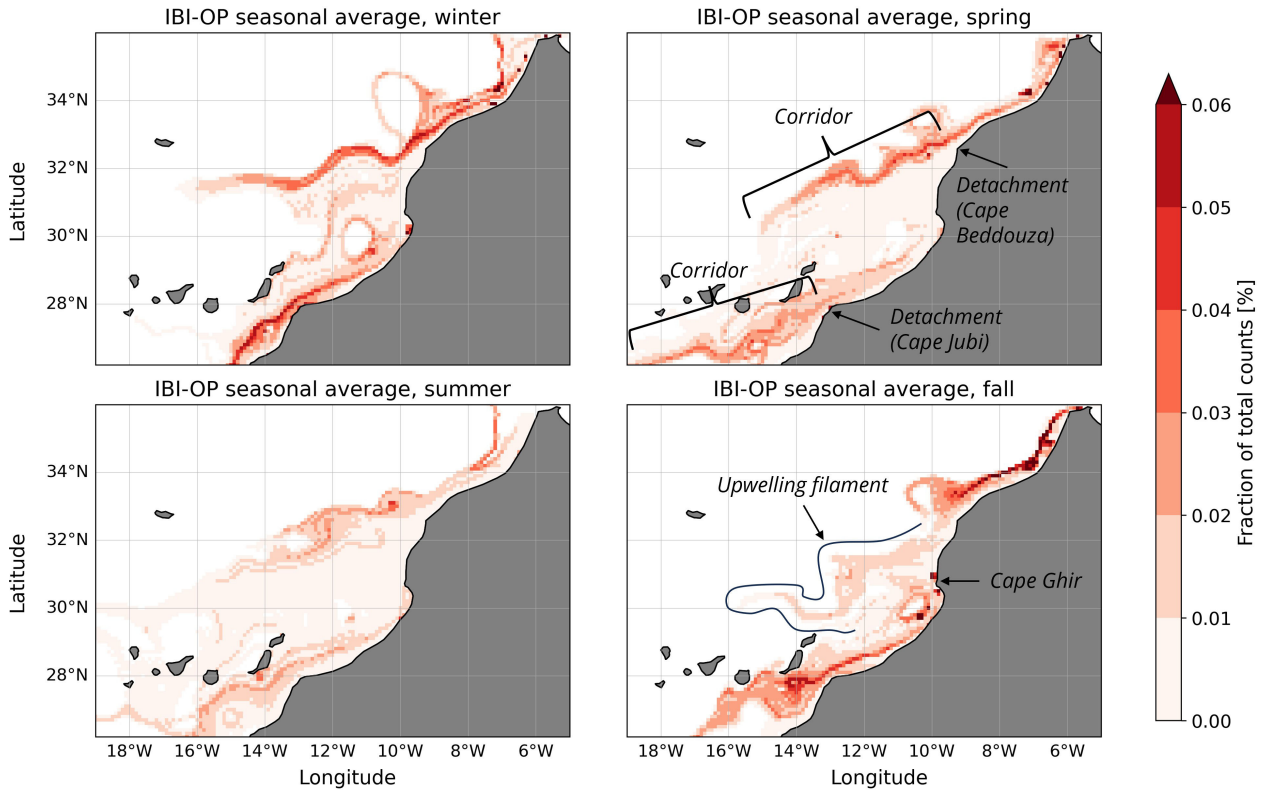


FIGURE 3
PDPs derived from the IBI-OP seasonal mean surface velocities for all seasons, defined in section 2.3.1, showing oceanward-oriented corridors during winter, spring and summer. The presence of the corridors and the locations of coastal particle detachment are indicated during the spring season. During autumn, a filament-shaped feature is observed at Cape Ghir and appears responsible for transporting particles oceanward.

details and visualization provided in the Supplementary Material (Supplementary Figure 1).

To assess the contributions of geostrophic and wind-driven dynamics, PDPs derived from simulations using AVISO and GlobCurrent seasonal climatology during spring are presented in Figure 5. Results for the other seasons, which exhibit similar patterns, are included in the Supplementary Material (Supplementary Figures 2, 3). The simulations using AVISO surface velocities produce markedly different results, showing particle retention along the African coast instead of the offshore transport associated with the previously described corridors. In contrast, the PDPs obtained using the GlobCurrent combined wind-driven and geostrophic surface dynamics clearly indicate the presence of the corridors, highlighting their critical role in facilitating oceanward transport of particles. The properties of the corridors using the GlobCurrent product are described in Table 2 for all seasons.

To investigate the vertical structure of features responsible for oceanward particle transport, particle trajectories obtained from simulations using the IBI-OP seasonal mean circulation during spring are shown in Figure 6 for four depths: 0, 22, 40, and 110 meters. Unlike PDPs, particle trajectories are displayed to provide detailed flow patterns and directional information within the structures. For clarity, Figure 6 also indicates the origin of particles using color coding and focuses specifically on the spring season, as it prominently displays the distinct Cape Ghir Corridor and filament-shaped oceanward transport at greater depths. Results for other seasons are included in the Supplementary Material (Supplementary Figures 4-6).

Figure 6 illustrates that particles transported oceanward by the corridors remain confined to depths shallower than 22 meters, identifying these features as predominantly surface-level structures. The filament-shaped transport is most prominent at 22 meters, diminishing in influence at depths beyond 40 meters. Despite the corridor's limited vertical extent, particles continue to move southward along the coast at 40 meters depth. At the surface, the corridor predominantly transports particles originating north of Cape Beddouza, while the filament-shaped structure primarily facilitates transport of particles originating between Cape Beddouza and Cape Ghir. However, from about 22 to about 40 meters depth, where the corridor dissipates but the filament-shaped structure remains active, it transports particles originating from the entire region north of Cape Ghir.

## 3.2 Daily varying surface velocities

PDPs derived from the IBI-OP daily varying surface velocities are presented in Figure 7 for all seasons. Despite the increased dispersion of particles, the corridors remain visible during winter, spring, and summer, with orientations similar to those observed in the simulations using seasonal mean surface velocities. For clarity, the corridor during the spring season is marked by two dashed lines in Figure 7. During autumn, a corridor is identified as well, although the zone of high particle counts is more fragmented and discontinuous. Moreover, compared to the simulations using seasonal mean surface circulation, there is a higher concentration of particles in the area just

TABLE 2 An overview of key parameters analytically describing the Cape Ghir Corridors, derived from various simulations.

| Product | Averaging method | Estimated max. speed coastal jet [m/s] | Estimated speed corridor [m/s] | Detachment angle [°] | Rossby number [-] |
|---|---|---|---|---|---|
| IBI-OP | Winter averaged over 2022 | 0.13 | 0.10 | 20 | 3.1 |
| IBI-OP | Spring averaged over 2022 | 0.21 | 0.09 | 23 | 2.8 |
| IBI-OP | Summer averaged over 2022 | 0.32 | 0.08 | 18 | 2.5 |
| IBI-OP | Autumn averaged over 2022 | No corridor | No corridor | No corridor | No corridor |
| GLORYS | Winter averaged over 1993 - 2020 | 0.10 | 0.07 | 40 | 2.2 |
| GLORYS | Spring averaged over 1993 - 2020 | 0.20 | 0.10 | 40 | 3.1 |
| GLORYS | Summer averaged over 1993 - 2020 | 0.27 | 0.10 | 31 | 3.1 |
| GLORYS | Autumn averaged over 1993 - 2020 | 0.09 | 0.06 | 26 | 1.9 |
| GlobCurrent | Winter averaged over 1993 - 2020 | 0.06 | 0.08 | 42 | 2.5 |
| GlobCurrent | Spring averaged over 1993 - 2020 | 0.11 | 0.12 | 40 | 3.9 |
| GlobCurrent | Summer averaged over 1993 - 2020 | 0.17 | 0.13 | 26 | 4.1 |
| GlobCurrent | Autumn averaged over 1993 - 2020 | 0.06 | 0.07 | 28 | 2.2 |

These parameters include the estimated speed of the coastal jet, the estimated speed of the corridor, and the detachment angle. The methodology used to compute these parameters is visually depicted in Figure 4. Moreover, the Rossby number is computed for each corridor as well, by dividing the estimated speed of the corridor by its general length (400 kilometers) times the appropriate Coriolis parameter ($8 \cdot 10^{-5}$ $s^{-1}$).

south of the Canary Islands, as observable from the darker red patches at this location.

The PDPs derived using the combined IBI-OP and IBI-OW products are presented in Figure 8. Notably, the oceanward transport is reduced compared to simulations without Stokes drift, as observable from the general absence of particles further away from the coast. However, some oceanward transport is still present, particularly during autumn. Nevertheless, particles appear to remain more confined along the coast and tend to flow through the Lanzarot passage when including Stokes drift. Also, the

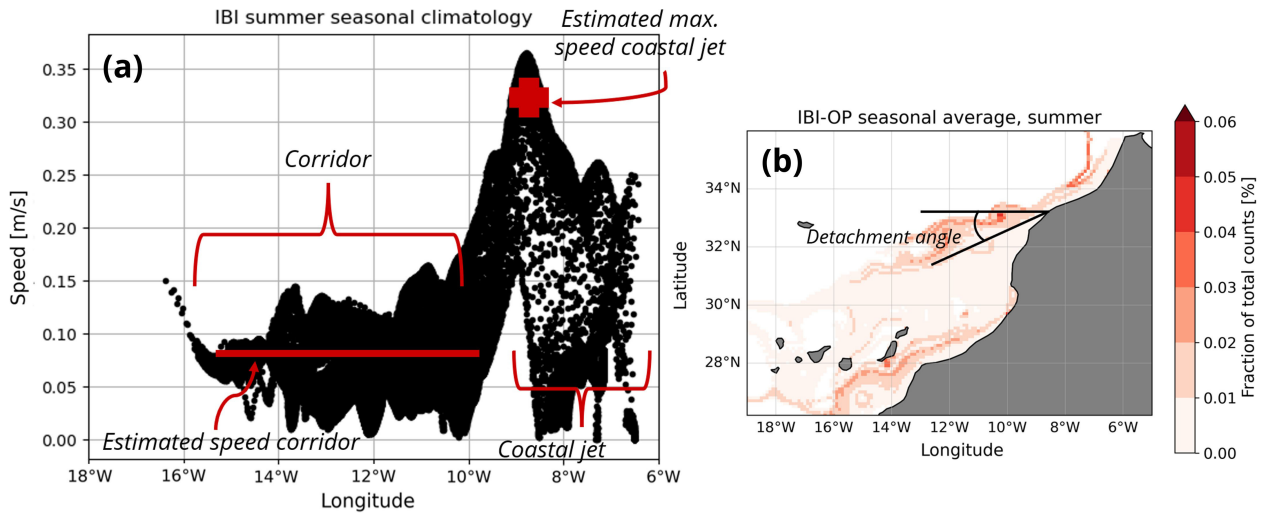


FIGURE 4
**(a)** Speed of particles released between 33°N and 35°N as a function of longitude, using the IBI-OP seasonal mean surface velocities during summer. It shows the methodology of estimating the maximum speed of the coastal jet stream and of the corridor. **(b)** PDP obtained from the same surface circulation, illustrating the method used to determine the detachment angle of the corridor.

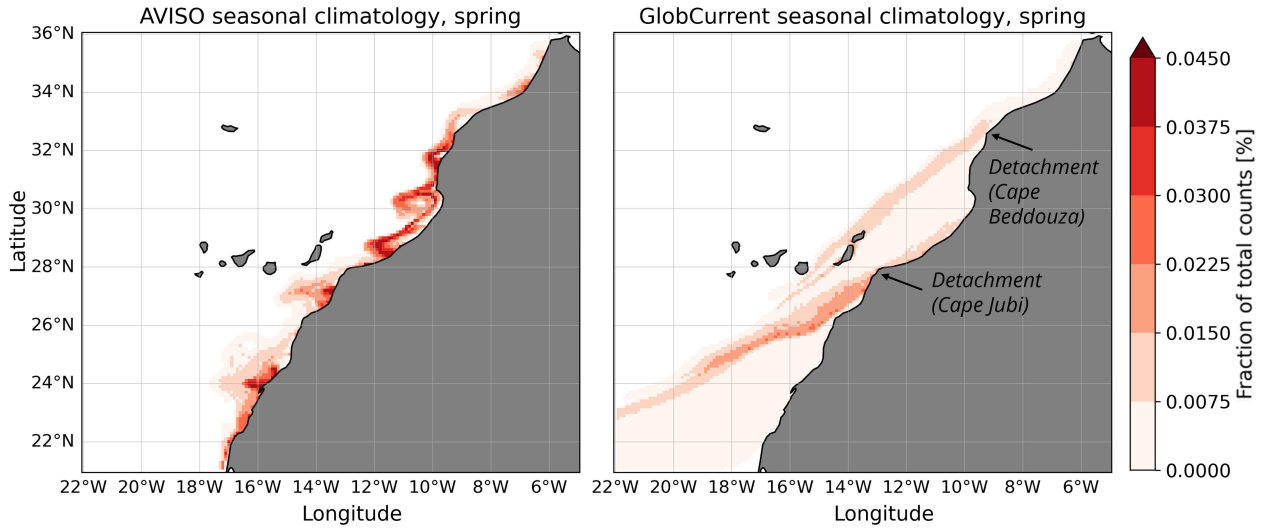


FIGURE 5
PDPs obtained using the AVISO and GlobCurrent seasonal mean surface velocities during spring, defined in section 2.3.1, reveal contrasting outcomes. Simulations with AVISO display a distinct retention of particles along the coast, while those using GlobCurrent again confirm the presence of the corridors facilitating oceanward transport. Similar patterns are observed across the other seasons in these simulations.

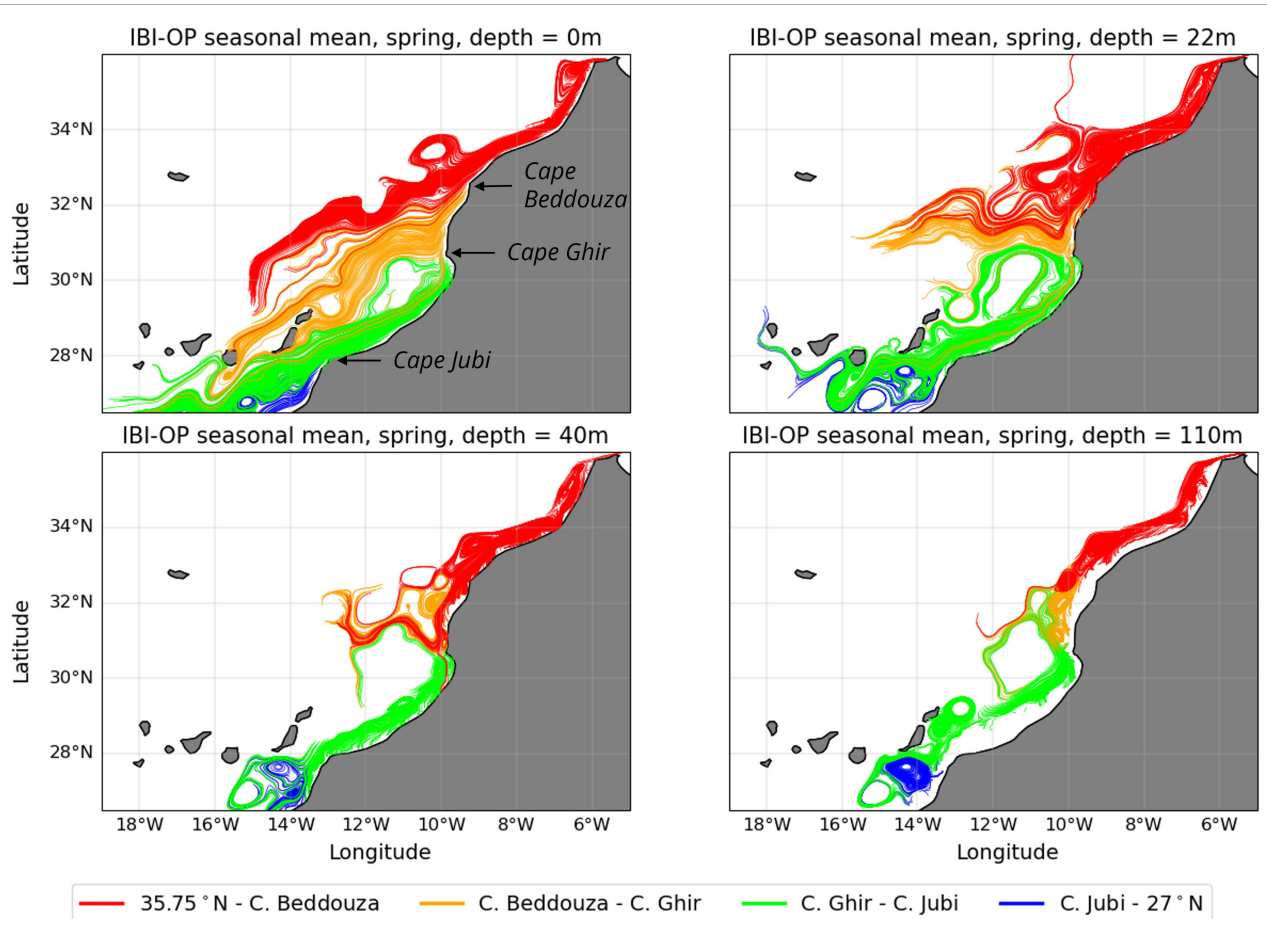


FIGURE 6
The horizontal trajectories of particles released at depths of 0, 22, 40 and 110 meters during spring, using the IBI-OP seasonal mean velocities, defined in section 2.3.1. The colors of the trajectories represent the subsequent areas of release: red: 35.75°N - Cape Beddouza, orange: Cape Beddouza - Cape Ghir, green: Cape Ghir - Cape Jubi, blue: Cape Jubi - 27°N.

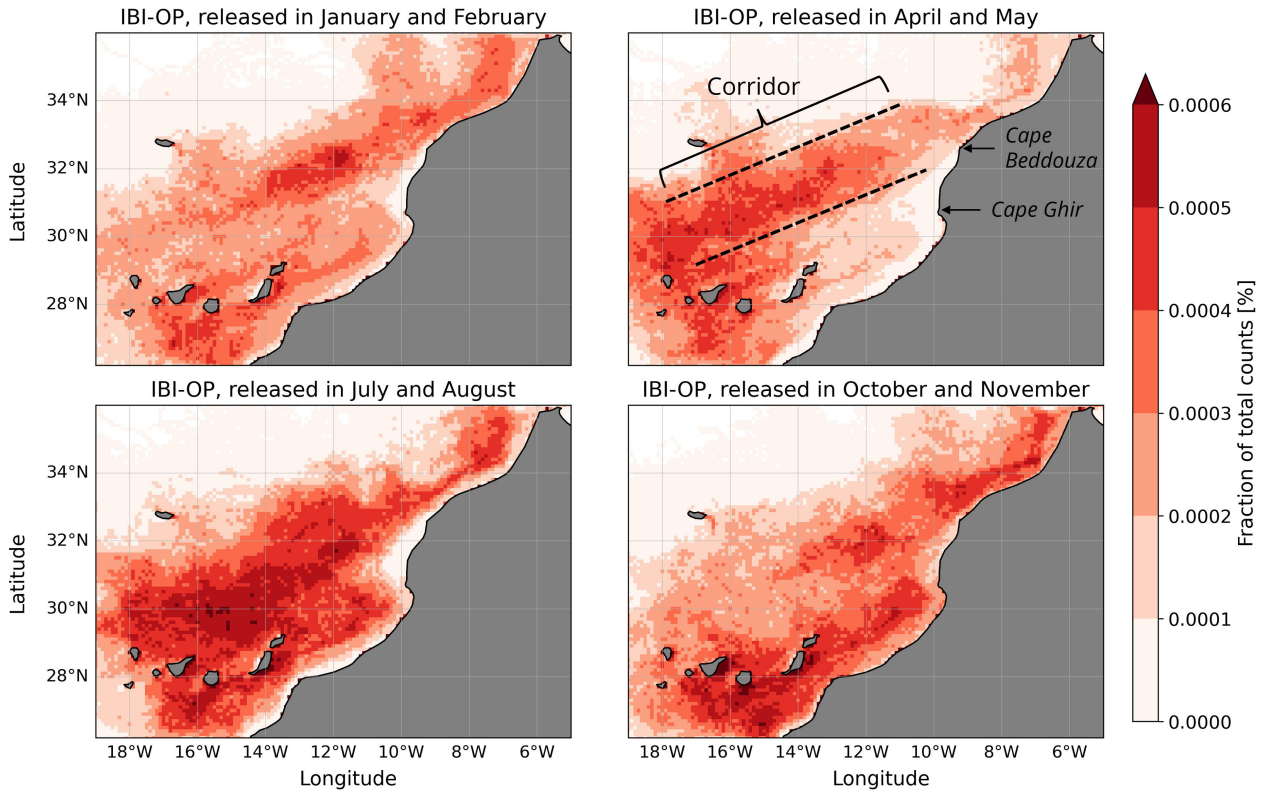


FIGURE 7
PDPs obtained using the IBI-OP daily variable surface velocities, defined in section 2.3.2. The simulation shows the corridors, although less profound compared to those derived from seasonal mean surface velocities, caused by the higher dispersion of probability in this Figure. For clarity, the Cape Ghir Corridor is highlighted during the spring season.

previously observed higher concentration of particles south of Gran Canaria and Tenerife is absent in this simulation.

# 4 Discussion

The formation of the major oceanward-transporting mechanisms will be discussed in Section 4.1, followed by the impact of Stokes drift in Section 4.2. Section 4.3 outlines the research limitations of this study and offers suggestions for future research. Finally, Section 4.4 synthesizes the main factors influencing oceanward transport from the release band.

## 4.1 Identification and formation of oceanward-transporting mechanisms

The simulations indicate the emergence of oceanward-oriented particle corridors originating from major capes along the release band, which have not, to our knowledge, been explicitly demonstrated in this region using Lagrangian tracking. Simulations using the AVISO product (Figure 5) indicate that the corridors are not present when only considering geostrophic circulation, as evidenced by their absence in these simulations. This observation is further supported by the lack of corridors at deeper levels (Figure 6), where geostrophic circulation predominates. Additionally, the high Rossby numbers associated with the corridors (Table 2) confirm their origin not to be purely geostrophic as well. In contrast, simulations using the GlobCurrent product (Figure 5), which incorporate wind-driven currents, clearly show the presence of these corridors. This highlights the critical role of wind-driven dynamics in their formation.

An important feature of these corridors is their shared characteristics. First, the corridors consistently originate from distinct capes along the coast. Second, they emerge north of an upwelling filament. This spatial relationship might initially suggest that the corridors are a result of oceanward transport induced by the filaments. However, closer examination indicates that the coastal detachment of particles occurs north of the upwelling filaments. Additionally, oceanward transport driven by a filament is often represented by a filament-shaped transport signature, as observed in Figure 3 during autumn or Figure 6 at a depth of 22 meters. These observations strongly indicate that the upwelling filaments are not directly responsible for the formation of the corridors. In addition to understanding the formation of the corridors, Troupin et al. (2012) suggests that the formation of the Cape Ghir Filament is likely driven by the detachment of the coastal jet stream. This detachment is partially caused by the addition of potential vorticity near the cape, which forces the jet stream oceanward. Subsequently, an upwelling filament may generate variations in the thermohaline properties of the surrounding waters, potentially triggering dynamic processes in the vicinity of the filament. To gain a more detailed understanding about the role of this coastal jet stream in oceanward particle transport, Figure 9 illustrates surface speeds around Cape

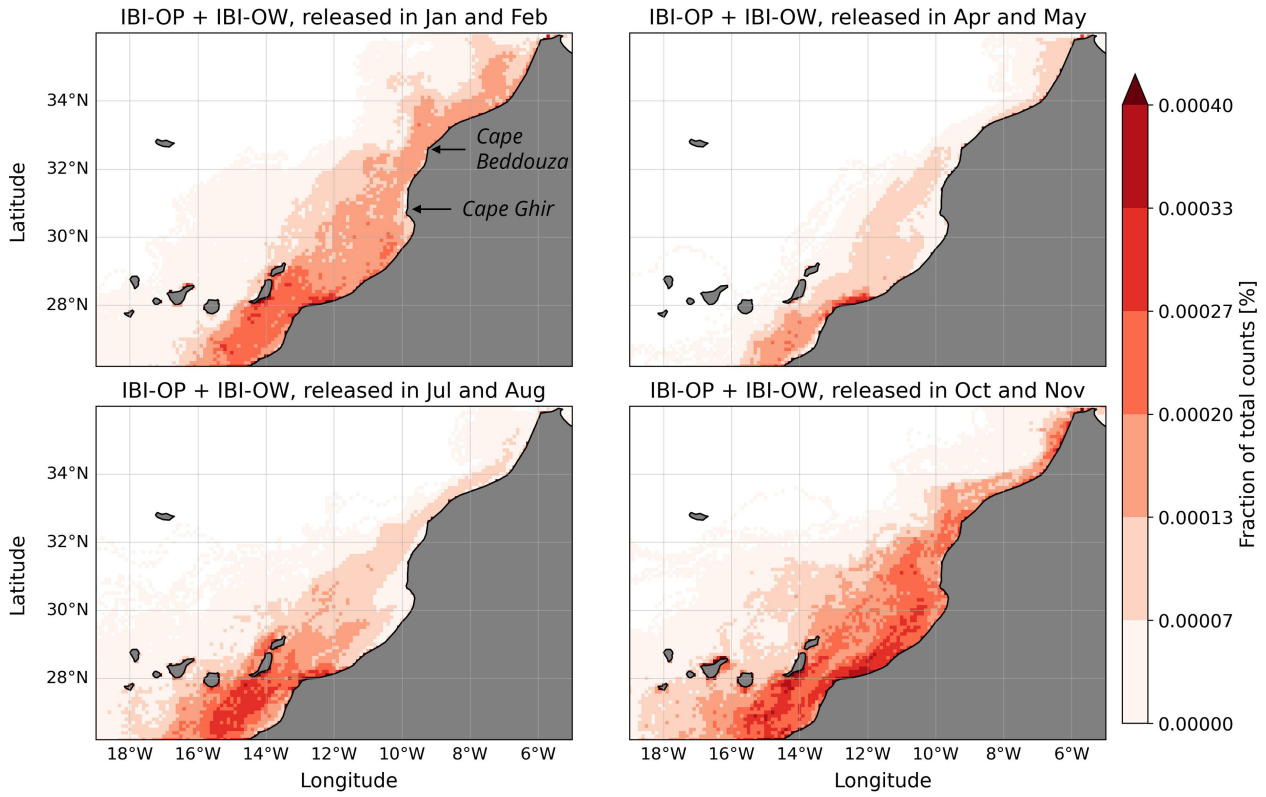


FIGURE 8
PDPs obtained using the IBI-OP + IBI-OW daily variable surface velocities for the four seasons, defined in section 2.3.2. The particles are generally prevented from being transported oceanward and the oceanward corridors appear to be absent as well. Nevertheless, some oceanward transport is still observed north of Lanzarote, particularly during autumn.

Beddouza on selected days, indicating variations in jet stream behavior. On days with a strong coastal jet stream, it clearly detaches from the coast (panels a and b). On a day with a weaker jet stream, it detaches weakly (panel c), while on a day without a coastal jet stream, no detachment occurs (panel d). Additionally, the trajectories of particles released north of Cape Beddouza (red) and between Cape Beddouza and Cape Ghir (orange) are superimposed, further illustrating the relationship between particle transport and coastal jet dynamics. The detachment of the coastal jet is hypothesized to be the primary mechanism driving the formation of the observed corridors. This hypothesis is supported by the observation that particles consistently follow the jet stream and detach at the same locations where the jet stream itself detaches from the coast. This pattern is evident not only in Figure 9 but also in other simulations, such as those depicted in Figures 3, 5, 6, where the particles detach just north of Cape Beddouza as well. In addition to the jet stream detachment, the Cape Ghir filament is also visible in the surface speed data from Figure 9, characterized by oceanward-oriented patches of higher velocity. Particles are transported by this filament, showing its potential of transporting particles oceanward as well.

Strengthening the hypothesis that jet detachment is an important driver of oceanward particle transport, particles are transported only weakly oceanward during conditions with a weak jet stream, whereafter they merge with the particles transported by the filament (Figure 9c). Furthermore, during the absence of a jet stream, particles move slowly and remain near the coast (Figure 9d). Moreover, Figure 9 demonstrates that stronger jet streams are associated with enhanced oceanward advection by the upwelling filament. This observation aligns with the findings of Troupin et al. (2012), which emphasize the strong interconnection between the upwelling filament and the jet stream.

However, the mechanism underlying the detachment of the coastal jet remains an unresolved question. According to Troupin et al. (2012), this detachment may be driven by the addition of vorticity from the regional wind field, which forces the jet to flow along greater depths further from the coast. Alternatively, another mechanism potentially causing the detachment of the jet is inertial overshoot, since fast-flowing coastal currents might tend to separate from the coast at major capes by this process (Pierini et al., 2011; Ou and Ruijter, 1986). Regardless of whether the detachment is due to inertial overshoot or another mechanism, the results in Figure 9 demonstrate that oceanward particle transport is closely tied to the strength of the coastal jet stream, impacting the severity of coastal jet detachment, creating the previously observed particle corridors, and likely the strength of the upwelling filament too. This further highlights its central role in particle transport dynamics.

It is noteworthy that, although the corridors are likely not directly formed by upwelling filaments, the filaments remain closely associated with the detachment of the coastal jet stream and, consequently, with the formation of the corridors. Moreover, the upwelling filaments themselves contribute substantially to the oceanward transport of particles. This linkage is evident from the surface particle trajectories obtained using the IBI-OP seasonal

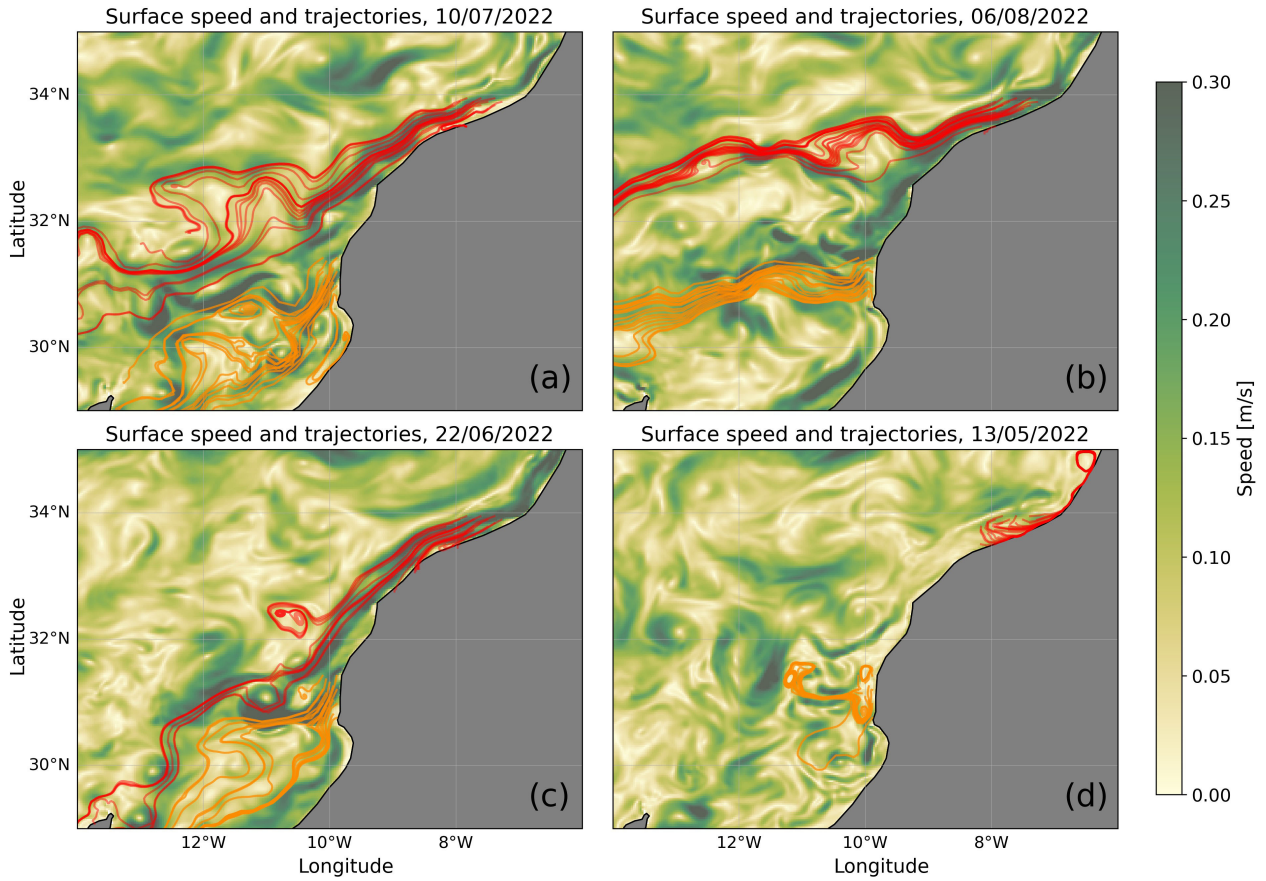


FIGURE 9
The surface speed from the IBI-OP product for four individual days, with the trajectories of particles released just north of Cape Beddouza (red) and just north of Cape Ghir (orange) superimposed. Panels **(a, b)** show the presence of the coastal jet stream, along with its coastal detachment, causing the particles to detach from the coast at the same location. Additionally, oceanward-oriented patches of high speed indicate the presence of the Cape Ghir Filament, which also transports particles offshore. In contrast, panels **(c, d)** depict conditions with a weak or absent jet stream and reduced filament activity. These conditions result in minimal or no oceanward transport of particles, highlighting the critical role of both the jet stream and filament in driving offshore particle movement.

average (Figure 6). In this figure, particles released between Cape Beddouza and Cape Ghir, within the region influenced by the Cape Ghir Filament, are transported oceanward nearly as effectively as those released north of Cape Beddouza, which are primarily transported via the Cape Ghir Corridor. Furthermore, the upwelling filament appears to play a prominent role in transporting particles at depths between approximately 20 and 40 meters, as illustrated in Figure 6. These observations suggest that the Cape Ghir Filament, along with potentially other filaments within the study domain, constitutes an important mechanism for oceanward particle transport, highlighting the complementary roles of the filaments and corridors in driving offshore transport dynamics.

## 4.2 The role of Stokes drift

To evaluate the effect of Stokes drift, Figure 10 presents the seasonal mean velocity fields for IBI-OP, IBI-OW, and the combined IBI-OP + IBI-OW during spring. These velocity fields indicate that, while Stokes drift is not necessarily dominant across all locations, it introduces a consistent southward velocity component. Since this southward velocity aligns with the southward background flow driven by the Canary Current (CC), Stokes drift enhances the southward component of the regional flow in the conducted simulations. Moreover, Figure 10 indicates that Stokes drift velocities tend to bend slightly toward the shore upon approaching the coastline, enhancing the potential for particles to become trapped along the shore.

When examining the PDPs obtained without any averaging (Figure 8), a small yet notable number of particles are transported north of Lanzarote and reach other islands, including La Palma. This is likely influenced by the daily variability in Stokes drift as well as in the strength of the jet stream and upwelling filaments. It is proposed that during periods of relatively weak Stokes drift and/or strong jet stream conditions, particles are more likely to flow oceanward north of Lanzarote. Conversely, during periods of stronger Stokes drift or weaker jet stream conditions, particles tend to be transported through the Lanzarote passage.

It is also important to acknowledge, as noted in Section 2.3.1, that the exact method of incorporating Stokes drift remains an ongoing area of research and is likely overestimated in this study. Therefore, the inclusion of full Stokes drift should be interpreted as an upper-bound estimate and its quantitative impact on coastal retention may be overestimated. Reducing the Stokes drift

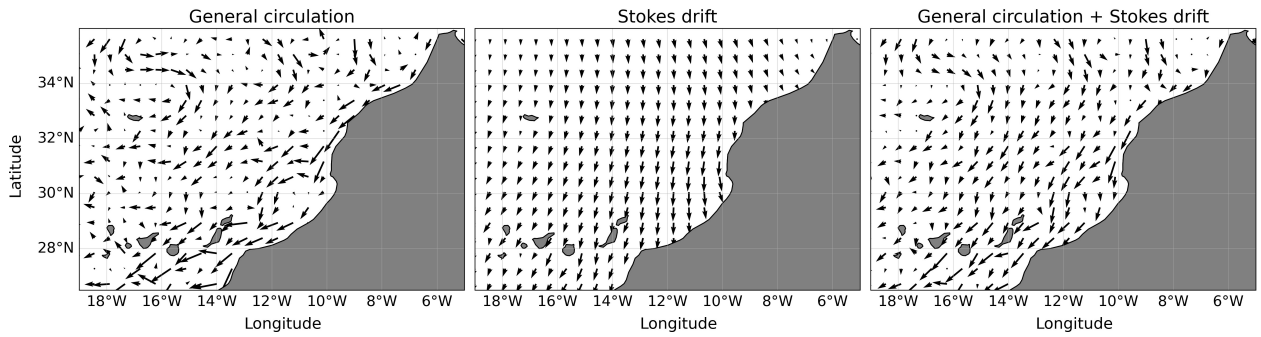


FIGURE 10
Vector plot of averaged surface velocity during spring derived from general circulation (IBI-OP, left), Stokes drift (IBI-OW, middle), and their combined effect (IBI-OP + IBI-OW, right). This Figure illustrates the constant and predominantly southward flow introduced by Stokes drift, which is observed for the other seasons as well.

contribution would likely weaken the southward deflection of the oceanward corridors and thus enhance their relative visibility and persistence. Nevertheless, even if Stokes drift were weaker in reality, its influence would likely reduce the overall oceanward transport of particles and, consequently, the number of particles potentially reaching the Canary Islands.

## 4.3 Research limitations and future research

Overall, this study applies OceanParcels to explore the oceanward transport of passive surface particles, with potential implications for marine litter transport from the African upwelling zone. The method has proven effective in identifying the key features responsible for facilitating oceanward transport. However, it is important to acknowledge that several research limitations may influence the accuracy of the results. This section will address these limitations and propose recommendations for future research to build upon the findings of this study.

It is important to highlight that, although the ocean products used in this study provide eddy-resolving spatial resolution and daily temporal resolution, they still rely on spatial and temporal parameterizations. As a result, they do not fully capture all processes that may influence surface circulation. Additionally, as previously discussed, Stokes drift is likely overestimated in this study. To obtain a more accurate assessment of the oceanward flux of particles, future research should employ more advanced methods for incorporating Stokes drift, as suggested by Higgins et al. (2020). An observational validation using GDP drifters or remote sensing products is beyond the scope of this study, but would be an important avenue for future research.

Also, one aspect that could impact the trajectories of marine litter specifically is the addition of windage (Cardoso and Caldeira, 2021; Iskandar et al., 2022). Windage is defined as the impact of wind on the movement of marine floating debris. The windage impact can be categorized by the type of debris, primarily based on its buoyancy (Duhec et al., 2015). However, although the exclusion of windage has minor impact on some types of marine litter and other particles present within the sea surface, the simulated trajectories are meant to represent passive water-following particles, since rather buoyant objects may exhibit substantially different pathways due to windage. Therefore, caution is required when extrapolating these results to buoyant marine litter. For future research, incorporating windage could provide a more detailed understanding of the trajectories of different categories of marine floating debris.

Moreover, this study does not examine oceanward transport facilitated by upwelling-generated eddies. These eddies have the capacity to capture and transport particles from the upwelling region into the open ocean, as demonstrated by García-Muñoz et al. (2004) and Vega-Moreno et al. (2021). OceanParcels shows the potential to be used in analyzing this transport by releasing particles in observed eddies, offering a detailed numerical analysis of their trajectories and broader understanding of their role in oceanward transport from the defined release band.

In addition, this study generalizes the entire upwelling zone with respect to marine pollution, which limits the representation of specific pollution sources. As a result, the simulated particle advection does not directly correspond to the transport of a certain amount of marine litter. In future research, integrating marine pollution data from specific locations within the upwelling zone could provide a more realistic representation of the actual transport of marine litter toward the Canary Islands.

## 4.4 Synthesis of the oceanward transport of particles from the upwelling zone

This section aims to synthesize all the mechanisms that contribute to the oceanward transport of particles from the upwelling zone identified in this study, as visualized in Figure 11.

Particles accumulate and flow southward along the shore driven by the coastal jet stream (1). These particles are likely to be transported oceanward by coastal jet stream detachment (2). However, the extent of this oceanward transport depends heavily on the balance between the strength of the jet stream during detachment and the influence of Stokes drift. If Stokes drift dominates, particle trajectories bend strongly southward, causing them to flow through the Lanzarote passage instead (4). Also, particles released south of Cape Beddouza but north of Cape Ghir are likely transported oceanward by the semi-permanent upwelling

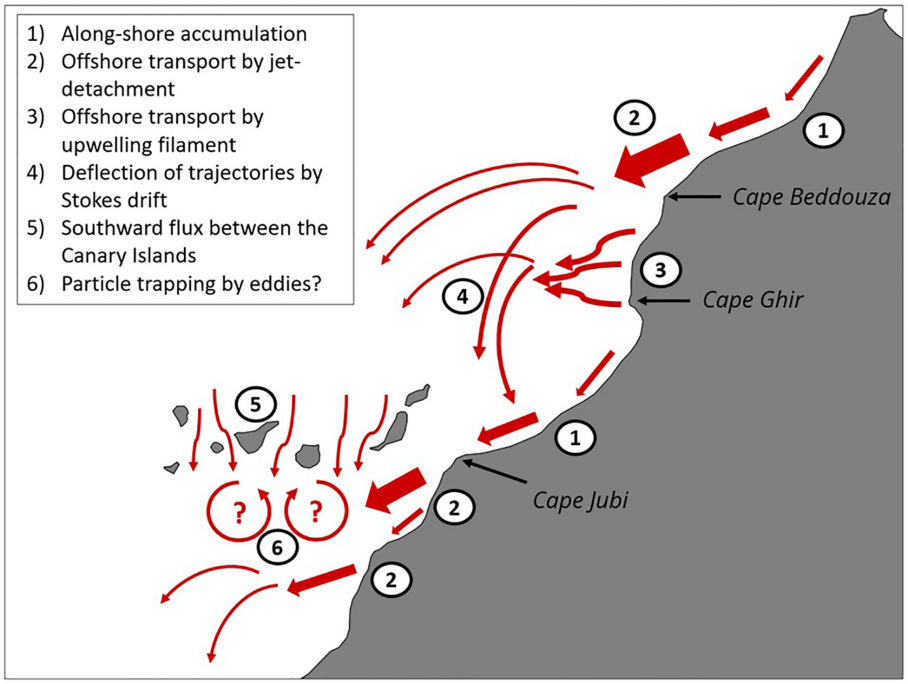


FIGURE 11
A visual synthesis of the oceanward transport of particles from the northwestern African upwelling zone, mainly covering the impact of jet detachment, filaments and Stokes drift.

filament (3). Again, the relative strengths of the filament and Stokes drift determine whether particles move north of Lanzarote toward the Canary Islands or through the Lanzarote passage (4). Nevertheless, for particles reaching the northern Canary Islands, the net southward flow caused by the Canary Current and Stokes drift is likely to transport them southward between the islands (5). As stated in section 4.3, upwelling-generated eddies may play a relevant role in the trapping and oceanward transport of particles south of the Canary Islands. This mechanism, however, requires further investigation in future research (6).

## 5 Conclusions

This study employed Lagrangian simulations forced by multiple ocean reanalysis and satellite-derived surface velocity products to examine oceanward transport from a coastal release band within the NW African upwelling system (27°N–35.75°N) and the mechanisms shaping the resulting particle pathways. The simulations indicate the emergence of coherent oceanward-oriented particle corridors in the model framework that have not been explicitly characterized in previous Lagrangian studies of this region. These structures extend several hundred kilometers in length and are largely confined to the upper 20 meters of the water column. The mechanism driving the formation of these corridors appears to be primarily wind-driven rather than geostrophic, as evidenced by their absence at greater depths and in simulations that include only geostrophic circulation. By comparing particle trajectories with surface speed patterns, this study suggests that the detachment of the coastal jet stream is a primary mechanism behind the formation of these corridors. Cape Ghir exhibits the best defined corridor, although its presence seems to be rather vague during autumn. The Cape Ghir Filament, and potentially other upwelling filaments, also represent important mechanisms in the oceanward transport of particles, despite the reduced particle input to the filament caused by earlier oceanward transport through jet stream detachment. Its influence is particularly present during autumn.

The simulations indicate that Stokes drift influences particle trajectories, acting as a counterforce to oceanward transport. In the model framework, Stokes drift introduces a southward velocity component that can drive detached particles back toward the coast. Moreover, its coastward deflection near the coast enhances the potential to reduce oceanward transport. Despite its influence across all seasons, the extent to which Stokes drift affects oceanward transport likely depends on the daily balance between the strength of Stokes drift and the features that facilitate oceanward particle movement, such as the coastal jet stream and upwelling filaments. This interplay determines the overall modulation of oceanward transport.

These findings are consistent with the hypothesis that the northwestern African upwelling zone may contribute to the offshore export of surface material toward the Canary Islands. Multiple mechanisms identified in this study, such as coastal jet detachment and upwelling filaments, highlight their potential to organize offshore surface transport. However, the role of windage, the transport of particles by upwelling-generated eddies, and marine pollution data should be incorporated to further constrain this hypothesis.

## Data availability statement

The original contributions presented in the study are included in the article/supplementary material. Details on the datasets, repositories, and algorithms used are provided in the Data and Methods section. Further inquiries can be directed to the corresponding authors.

## Author contributions

LR: Data curation, Visualization, Methodology, Formal analysis, Conceptualization, Writing – original draft, Writing – review & editing. BA-G: Conceptualization, Methodology, Project administration, Supervision, Writing – review & editing, Visualization, Formal analysis, Funding acquisition. TP: Writing – review & editing, Project administration, Supervision. DV-M: Conceptualization, Writing – review & editing, Project administration. EF-N: Writing – review & editing, Project administration, Conceptualization. FM: Writing – review & editing, Formal analysis, Methodology, Supervision, Visualization, Conceptualization.

## Funding

The author(s) declared that financial support was received for this work and/or its publication. BA-G acknowledges support from the Spanish Government (Ministerio de Ciencia, Innovación y Universidades) through the COUPLING II project (PID2023-148583NB-C21).

## Acknowledgments

The first author is grateful to the Erasmus+ Programme of the European Union, which financially supported his internship at ULPGC and IEO-CSIC, where this research was developed. The authors also thank the OceanParcels team for providing the Lagrangian framework used in this study (www.oceanparcels.org). We are grateful to the two reviewers for their careful reading of the manuscript and their insightful comments, which helped to improve the quality of this work.

## Conflict of interest

The author(s) declared that this work was conducted in the absence of any commercial or financial relationships that could be construed as a potential conflict of interest.

The authors BA-G, FM declared that they were an editorial board member of Frontiers, at the time of submission. This had no impact on the peer review process and the final decision.

## Generative AI statement

The author(s) declared that generative AI was not used in the creation of this manuscript.

Any alternative text (alt text) provided alongside figures in this article has been generated by Frontiers with the support of artificial intelligence and reasonable efforts have been made to ensure accuracy, including review by the authors wherever possible. If you identify any issues, please contact us.

## Publisher's note



## Supplementary material

The Supplementary Material for this article can be found online at: https://www.frontiersin.org/articles/10.3389/fmars.2026.1757436/full#supplementary-material

SUPPLEMENTARY FIGURE 1
PDPs obtained using the GLORYS seasonal mean surface circulation for all seasons, defined in section 2.3.1, confirming the presence of the corridors during winter, spring and summer.

SUPPLEMENTARY FIGURE 2
PDPs obtained using the AVISO seasonal mean surface circulation for all seasons, defined in section 2.3.1, only considering geostrophic surface dynamics.

SUPPLEMENTARY FIGURE 3
PDPs obtained using the GlobCurrent seasonal mean surface circulation for all seasons, defined in section 2.3.1, considering both geostrophic and wind-driven surface dynamics.

SUPPLEMENTARY FIGURE 4
The horizontal trajectories of particles released at depths of 0, 22, 40 and 110 meters during winter using the IBI-OP seasonal mean surface circulation, defined in section 2.3.1. The colors of the trajectories represent the subsequent areas of release: red: 35.75°N - Cape Beddouza, orange: Cape Beddouza - Cape Ghir, green: Cape Ghir - Cape Jubi, blue: Cape Jubi - 27°N.

SUPPLEMENTARY FIGURE 5
The horizontal trajectories of particles released at depths of 0, 22, 40 and 110 meters during summer using the IBI-OP seasonal mean surface circulation, defined in section 2.3.1. The colors of the trajectories represent the subsequent areas of release: red: 35.75° N - Cape Beddouza, orange: Cape Beddouza - Cape Ghir, green: Cape Ghir - Cape Jubi, blue: Cape Jubi - 27°N.

SUPPLEMENTARY FIGURE 6
The horizontal trajectories of particles released at depths of 0, 22, 40 and 110 meters during autumn using the IBI-OP seasonal mean surface circulation, defined in section 2.3.1. The colors of the trajectories represent the subsequent areas of release: red: 35.75° N - Cape Beddouza, orange: Cape Beddouza - Cape Ghir, green: Cape Ghir - Cape Jubi, blue: Cape Jubi - 27°N.

# References


Arístegui, J., Sangrá, P., Hernández-León, S., Cantón, M., Hernández-Guerra, A., and Kerling, J. L. (1994). Island-induced eddies in the Canary islands. *Deep. Sea. Res. Part I.: Oceanogr. Res. Pap.* 41, 1509–1525. doi: 10.1016/0967-0637(94)90058-2

Aznar, R., Sotillo, M. G., Cailleau, S., Lorente, P., Levier, B., Amo-Baladrón, A., et al. (2016). Strengths and weaknesses of the CMEMS forecasted and reanalyzed solutions for the Iberia–Biscay–Ireland (IBI) waters. *J. Mar. Syst.* 159, 1–14. doi: 10.1016/j.jmarsys.2016.02.007

Barton, E. D., Arıstegui, J., Tett, P., Cantón, M., Garcıa-Braun, J., Hernández-León, S., et al. (1998). The transition zone of the Canary Current upwelling region. *Prog. Oceanogr.* 41, 455–504. doi: 10.1016/S0079-6611(98)00023-8

Baztan, J., Carrasco, A., Chouinard, O., Cleaud, M., Gabaldon, J. E., Huck, T., et al. (2014). Protected areas in the Atlantic facing the hazards of micro-plastic pollution: First diagnosis of three islands in the Canary Current. *Mar. pollut. Bull.* 80, 302–311. doi: 10.1016/j.marpolbul.2013.12.052

Benazzouz, A., Mordane, S., Orbi, A., Chagdali, M., Hilmi, K., Atillah, A., et al. (2014). An improved coastal upwelling index from sea surface temperature using satellite-based approach – The case of the Canary Current upwelling system. *Continent. Shelf. Res.* 81, 38–54. doi: 10.1016/j.csr.2014.03.012

Breivik, Ø., Bidlot, J.-R., and Janssen, P. A. E. M. (2016). A stokes drift approximation based on the phillips spectrum. *Ocean. Model.* 100, 49–56. doi: 10.1016/j.ocemod.2016.01.005

Cardoso, C., and Caldeira, R. M. A. (2021). Modeling the exposure of the macaronesia islands (NE atlantic) to marine plastic pollution. *Front. Mar. Sci.* 8. doi: 10.3389/fmars.2021.653502

Chiswell, S. M., and Rickard, G. J. (2008). Eulerian and Lagrangian statistics in the Bluelink numerical model and AVISO altimetry: Validation of model eddy kinetics. *J. Geophys. Res.: Ocean.* 113, C10. doi: 10.1029/2007JC004673

Cividanes, M., Aguiar-González, B., Gómez, M., Herrera, A., Martínez, I., Pham, C., et al. (2024). Lagrangian tracking of long-lasting plastic tags: From lobster fisheries in the usa and Canada to macaronesia. *Mar. pollut. Bull.* 198, 115908. doi: 10.1016/j.marpolbul.2023.115908

Cunningham, H. J., Higgins, C., and van den Bremer, T. S. (2022). The role of the unsteady surface wave-driven ekman–stokes flow in the accumulation of floating marine litter. *J. Geophys. Res.: Ocean.* 127, e2021JC018106. doi: 10.1029/2021JC018106

Delandmeter, P., and van Sebille, E. (2019). The Parcels v2.0 Lagrangian framework: new field interpolation schemes. *Geosci. Model. Dev.* 12, 3571–3584. doi: 10.5194/gmd-12-3571-2019

Duhec, A. V., Jeanne, R. F., Maximenko, N., and Hafner, J. (2015). Composition and potential origin of marine debris stranded in the Western Indian Ocean on remote Alphonse Island, Seychelles. *Mar. pollut. Bull.* 96, 76–86. doi: 10.1016/j.marpolbul.2015.05.042

García-Muñoz, M., Arístegui, J., Montero, M. F., and Barton, E. D. (2004). Distribution and transport of organic matter along a filament-eddy system in the Canaries – NW Africa coastal transition zone region. *Prog. Oceanogr.* 62, 115–129. doi: 10.1016/j.pocean.2004.07.005

Hernández-Sánchez, C., González-Sálamo, J., Díaz-Peña, F. J., Fraile-Nuez, E., and Hernández-Borges, J. (2021). Arenas Blancas (El Hierro island), a new hotspot of plastic debris in the Canary Islands (Spain). *Mar. pollut. Bull.* 169, 112548. doi: 10.1016/j.marpolbul.2021.112548

Hersbach, H., Bell, B., Berrisford, P., Hirahara, S., Horányi, A., Muñoz-Sabater, J., et al. (2020). The ERA5 global reanalysis. *Q. J. R. Meteorol. Soc.* 146, 1999–2049. doi: 10.1002/qj.3803

Higgins, C., Vanneste, J., and Van Den Bremer, T. S. (2020). Unsteady Ekman-Stokes dynamics: implications for surface wave-induced drift of floating marine litter. *Geophys. Res. Lett.* 47, e2020GL089189. doi: 10.1029/2020GL089189

Iskandar, M. R., Cordova, M. R., and Park, Y.-G. (2022). Pathways and destinations of floating marine plastic debris from 10 major rivers in Java and Bali, Indonesia: A Lagrangian particle tracking perspective. *Mar. pollut. Bull.* 185, 114331. doi: 10.1016/j.marpolbul.2022.114331

Lange, M., and van Sebille, E. (2017). Parcels v0.9: prototyping a Lagrangian ocean analysis framework for the petascale age. *Geosci. Model. Dev.* 10, 4175–4186. doi: 10.5194/gmd-10-4175-2017

Lathuilière, C., Echevin, V., and Lévy, M. (2008). Seasonal and intraseasonal surface chlorophyll-a variability along the northwest African coast. *J. Geophys. Res.: Ocean.* 113, C10. doi: 10.1029/2007JC004433

Law-Chune, S., Aouf, L., Dalphinet, A., Levier, B., Drillet, Y., and Drevillon, M. (2021). WAVERYS: a CMEMS global wave reanalysis during the altimetry period. *Ocean. Dyn.* 71, 357–378. doi: 10.1007/s10236-020-01433-w

Lellouche, J.-M., Greiner, E., Le Galloudec, O., Garric, G., Regnier, C., Drevillon, M., et al. (2018). Recent updates to the Copernicus Marine Service global ocean monitoring and forecasting real-time 112° high-resolution system. *Ocean. Sci.* 14, 1093–1126. doi: 10.5194/os-14-1093-2018

Machín, F., Hernández-Guerra, A., and Pelegrí, J. (2006). Mass fluxes in the Canary Basin. *Prog. In. Oceanogr.* 70, 416–447. doi: 10.1016/j.pocean.2006.03.019

Madec, G., and the NEMO System Team (2024). *NEMO Ocean Engine Reference Manual*, Zenodo. doi: 10.5281/zenodo.1464816

Mason, E., Colas, F., and Pelegrí, J. (2012). A Lagrangian study tracing water parcel origins in the Canary Upwelling System. *Adv. Span. Phys. Oceanogr.* 76, 79–94. doi: 10.3989/scimar.03608.18D

Maximenko, N., Hafner, J., and Niiler, P. (2012). Pathways of marine debris from trajectories of Lagrangian drifters. *Mar. pollut. Bull.* 42, 51–62. doi: 10.1016/j.marpolbul.2011.04.016

Nieto, K., Demarcq, H., and McClatchie, S. (2012). Mesoscale frontal structures in the Canary Upwelling System: New front and filament detection algorithms applied to spatial and temporal patterns. *Remote Sens. Environ.* 123, 339–346. doi: 10.1016/j.rse.2012.03.028

Orós, J., Torrent, A., Calabuig, P., and Déniz, S. (2005). Diseases and causes of mortality among sea turtles stranded in the Canary Islands, Spain, (1998–2001). *Dis. Aquat. Organism.* 63, 13–24. doi: 10.3354/dao063013

Ou, H. W., and Ruijter, W. P. M. D. (1986). Separation of an inertial boundary current from a curved coastline. *J. Phys. Oceanogr.* 16, 280–289. doi: 10.1175/1520-0485(1986)016<0280:SOAIBC>2.0.CO;2

Pelegrí, J. L., Arístegui, J., Cana, L., González-Dávila, M., Hernández-Guerra, A., Hernández-León, S., et al. (2005). Coupling between the open ocean and the coastal upwelling region off northwest Africa: water recirculation and offshore pumping of organic matter. *J. Mar. Syst.* 54, 3–37. doi: 10.1016/j.jmarsys.2004.07.003

Pierini, S., Falco, P., Zambardino, G., McClimans, T. A., and Ellingsen, I. (2011). A laboratory study of nonlinear western boundary currents, with application to the Gulf Stream separation due to inertial overshooting. *J. Phys. Oceanogr.* 41, 2063–2079. doi: 10.1175/2011JPO4514.1

Rio, M.-H., Mulet, S., and Picot, N. (2014). Beyond GOCE for the ocean circulation estimate: Synergetic use of altimetry, gravimetry, and in *situ* data provides new insight into geostrophic and Ekman currents. *Geophys. Res. Lett.* 41, 8918–8925. doi: 10.1002/2014GL061773

Sala, I., Caldeira, R., Estrada-Allis, S., Froufe, E., and Couvelard, X. (2013). Lagrangian transport pathways in the northeast Atlantic and their environmental impact. *Fluids. Environ.* 3, 40–60. doi: 10.1215/21573689-2152611

Sangrà, P., Troupin, C., Barreiro-González, B., Barton, E., Orbi, A., and Arístegui, J. (2015). The Cape Ghir filament system in August 2009 (NW Africa). *J. Geophys. Res.* 120, 4516–4533. doi: 10.1002/2014JC010514

Santana-Falcón, Y., Mason, E., and Arístegui, J. (2020). Offshore transport of organic carbon by upwelling filaments in the Canary Current System. *Prog. Oceanogr.* 186, 102322. doi: 10.1016/j.pocean.2020.102322

Toledano, C., Ghantous, M., Lorente, P., Dalphinet, A., Aouf, L., and Sotillo, M. G. (2022). Impacts of an altimetric wave data assimilation scheme and currents-wave coupling in an operational wave system: the new copernicus marine IBI wave forecast service. *J. Mar. Sci. Eng.* 10, 457. doi: 10.3390/jmse10040457

Troupin, C., Mason, E., Beckers, J.-M., and Sangrà, P. (2012). Generation of the Cape Ghir upwelling filament: A numerical study. *Ocean. Model.* 41, 1–15. doi: 10.1016/j.ocemod.2011.09.001

Valdés, L., and Déniz-González, I. (2015). Oceanographic and biological features in the Canary Current Large Marine Ecosystem. *IOC. Tech. Ser.* 115, 383.

Van Den Bremer, T. S., and Breivik, Ø. (2017). Stokes drift. *Philos. Trans. R. Soc. A.: Math. Phys. Eng. Sci.* 376, 20170104. doi: 10.1098/rsta.2017.0104

van Sebille, E., Griffies, S. M., Abernathey, R., Adams, T. P., Berloff, P., Biastoch, A., et al. (2018). Lagrangian ocean analysis: Fundamentals and practices. *Ocean. Model.* 121, 49–75. doi: 10.1016/j.ocemod.2017.11.008

van Sebille, E., Aliani, S., Law, K. L., Maximenko, N., Alsina, J. M., Bagaev, A., et al. (2020). The physical oceanography of the transport of floating marine debris. *Environ. Res. Lett.* 15, 023003. doi: 10.1088/1748-9326/ab6d7d

Vega-Moreno, D., Abaroa-Pérez, B., Rein-Loring, P. D., Presas-Navarro, C., Fraile-Nuez, E., and Machín, F. (2021). Distribution and transport of microplastics in the upper 1150 m of the water column at the Eastern North Atlantic Subtropical Gyre, Canary Islands, Spain. *Sci. Tot. Environ.* 788, 147802. doi: 10.1016/j.scitotenv.2021.147802

Vega-Moreno, D., Sicilia-González, S., Domínguez-Hernández, C., Moreira-García, E., Aguiar-González, B., Hernández-Borges, J., et al. (2024). Exploring the origin and fate of surface and sub-surface marine microplastics in the Canary Islands region. *Front. Mar. Sci.* 1111. doi: 10.3389/fmars.2024.1314754

Villanova-Solano, C., Díaz-Peña, F. J., Hernández-Sánchez, C., González-Sálamo, J., González-Pleiter, M., Vega-Moreno, D., et al. (2022). Microplastic pollution in sublittoral coastal sediments of a North Atlantic island: The case of La Palma (Canary Islands, Spain). *Chemosphere* 288, 132530. doi: 10.1016/j.chemosphere.2021.132530